Nomura T Abe Y Kamada H Inoue M Kawara T Arita S Furuya T Yoshioka Y Shibata H Kayamuro H Yamashita T Nagano K Yoshikawa T Mukai Y Nakagawa S Taniai M Ohta T Tsunoda S Tsutsumi Y.	Novel protein engineering strategy for creating highly receptor-selective mutant TNFs	Biochem Biophys Res Commun	388	667-671	2009
Abe Y.	Development of novel DDS technologies for optimized protein therapy by creating functional mutant proteins with antagonistic activity	Yakugaku Zasshi	129	933-939	2009
Nomura T Abe Y Kamada H Inoue M Kawara T Arita S Furuya T Minowa K Yoshioka Y Shibata H Kayamuro H Yamashita T Nagano K Yoshikawa T Mukai Y Nakagawa S Tsunoda S Tsutsumi Y	Creation of an improved mutant TNF with TNFR1-selectivity and antagonistic activity by phage display technology	Pharmazie	65	93-96	2010

Chapter 33

Effective In Vitro and In Vivo Gene Delivery by the Combination of Liposomal Bubbles (Bubble Liposomes) and Ultrasound Exposure

Ryo Suzuki and Kazuo Maruyama

Abstract

Gene delivery with a physical mechanism using ultrasound (US) and nano/microbubbles is expected as an ideal system in terms of delivering plasmid DNA noninvasively into a specific target site. We developed novel liposomal bubbles (Bubble liposomes (BLs)) containing the lipid nanobubbles of perfluoropropane which were utilized for contrast enhancement in ultrasonography. BLs were smaller in diameter than conventional microbubbles and induced cavitation upon exposure ultrasound. In addition, when coupled with US exposure, BLs could deliver plasmid DNA into various types of cells in vitro and in vivo. The transfection efficiency with BLs and US was higher than that with conventional lipofection method. Therefore, the combination of BLs and US might be an efficient and novel nonviral gene delivery system.

Key words: Liposomes, Nanobubbles, Gene delivery, Ultrasound, Noninvasive, Nonviral vector

1. Introduction

Ultrasound (US) has been utilized as a useful tool for in vivo imaging, destruction of renal calculus and treatment for fibroid of the uterus. It was reported that US was proved to increase permeability of the plasma membrane and reduce the thickness of the unstirred layer of the cell surface, which encourages the DNA entry into cells (1, 2). The first studies applying ultrasound for gene delivery used frequencies in the range of 20–50 kHz (1, 3). However, these frequencies, along with cavitation, are also known to induce tissue damage if not properly controlled (4–6). To improve this problem, many studies using therapeutic ultrasound for gene delivery, which operates at frequencies of

Volkmar Weissig (ed.), *Liposomes*, Methods in Molecular Biology, vol. 605,
DOI 10.1007/978-1-60327-360-2_33, © Humana Press, a part of Springer Science+Business Media, LLC 2010

1–3 MHz, intensities of 0.5–2.5 W/cm^2, and pulse-mode have emerged (7–9). In addition, it was reported that the combination of therapeutic US and microbubble echo contrast agents could enhance gene transfection efficiency (10–14). In the sonoporation with microbubbles, it was reported that estimates of pore size based on the physical diameter of maker compounds were most commonly in the range of 30–100 nm, and estimates of membrane recovery time ranged from a few seconds to a few minutes (15). Therefore, it is thought that plasmid DNA is effectively and directly transferred into the cytosol via these pores. Conventional microbubbles including US contrast agents based on protein microspheres and sugar microbubbles are commercially available, the size of these bubbles being about 1–6 μm (16). For example, although the mean diameter of Optison microbubbles is about 2.0–4.5 μm, and they contain bubbles of up to 32 μm in diameter. Tsunoda et al. reported that some mice died immediately after the i.v. injection of Optison without ultrasound exposure due to lethal embolisms in vital organs (17). The same problem has not been reported in humans, but there is the possibility that Optison can not pass through capillary vessels. Therefore, microbubbles should generally be smaller than red blood cells. From this stand point of view, it is necessary to develop novel bubbles which are smaller than conventional microbubbles. Using liposome technology, we developed novel liposomal bubbles containing perfluoropropane gas. We called these bubbles "Bubble liposomes (BLs)." BLs were smaller than Optison (18–21). In addition, BLs could effectively deliver plasmid DNA by the combination with US exposure in vitro and in vivo.

2. Materials

2.1. Preparation of BLs (18)

1. 1,2-distearoyl-sn-glycero-phosphatidylcholone (DSPC) and 1,2-distearoyl-sn-glycero-3-phosphatidyl-ethanolamine-methoxypolyethyleneglycol (DSPE-PEG(2 k)-OMe) (NOF corporation, Tokyo, Japan).
2. Chloroform.
3. Diisopropyl ether.
4. Phosphate buffered saline (pH 7.4) (PBS): 137 mM NaCl, 8.10 mM Na_2HPO_4, 2.68 mM KCl, 1.47 mM KH_2PO_4 (Wako Pure Chemical Industries).
5. Perfluoropropane (Takachiho Chemical Industries, Tokyo, Japan).
6. Rotary evaporator (TOKYO RIKAKIKAI, Co. Ltd. (EYELA), Tokyo, Japan).

7. Extruding apparatus (Northern Lipids Inc., Vancouver, BC).
8. Bath-type sonicator (42 kHz, 100 W) (Branson Ultrasonics Co., Danbury, CT).
9. Liposome sizing filters (pore sizes: 100 and 200 nm) (Nuclepore Track-Etch Membrane, Whatman plc, UK).
10. 0.45 μm pore size filter (MILLEX HV filter unit, Durapore PVDF membrane) (Millipore Corporation, MA).
11. Dynamic light scattering (ELS-800) (Otsuka Electronics Co., Ltd., Osaka, Japan).
12. Phospholipid C-test wako (Wako Pure Chemical Industries).

2.2. Transmission Electron Microscopy of BLs (20)

1. Sodium alginate (500-600cP).
2. Calcium chloride.
3. Glutaraldehyde.
4. Cacodylate buffer.
5. Osmiumtetroxide.
6. Ethanol.
7. Epan812.
8. Uranyl acetate.
9. Electron microscope: JEOL JEM12000EX at 100 kV.

2.3. In Vitro Ultrasonography with BLs (19)

1. Ultrasound imaging equipment: UF-750XT (Fukuda Denshi Co. Ltd., Tokyo, Japan).
2. 9 MHz linear probe (9 MHz, Fukuda Denshi Co. Ltd.)

2.4. Gene Delivery with BLs and US In Vitro and In Vivo

1. Cells: COS-7 cells (the African green monkey kidney fibroblast cell line), S-180 cells (mouse sarcoma), Meth-A fibrosarcoma cells (mouse fibrosarcoma), Jurkat cells (human T cell line), Colon 26 cells (mouse colon adenocarcinoma), B16BL6 cells (mouse meranoma), Human umbilical vein endothelial cells (HUVEC) (Kurabo Industries, Osaka, Japan).
2. Culture media: Dulbecco's modified Eagle's medium (DMEM), RPMI-1640, Eagle's medium (MEM) and medium 199 (Sigma Chemical Co., St. Louis, MO), Supplements: Fetal bovine serum (FBS, GIBCO, Invitrogen Co., Carlsbad, CA), HEPES and heparin (Wako Pure Chemical Industries), endothelial cell growth supplement (ECGS) (Sigma Chemical Co.), Antibiotics: Penicillin and Streptomycin (Wako Pure Chemical Industries).
3. COS-7 cells and S-180 cells were cultured in DMEM supplemented with 10% heat-inactivated FBS. Meth-A fibrosarcoma cells and Jurkat cells were cultured with RPMI-1640 supplemented with 10% heat inactivated FBS. Colon 26 cells

were cultured with RPMI-1640 supplemented with 10% heat-inactivated FBS and 2.5% HEPES. B16BL6 cells were cultured with MEM supplemented with 10% heat-inactivated FBS. HUVECs were cultured in a DMEM and medium 199 mixture with 15% heat-inactivated FBS, heparin (3.25 U/mL) and ECGS. All culture media contained 100 U/ml penicillin and 100 μg/ml streptomycin.

4. Animals: ddY mice (4–6 weeks age, male), Anesthetic agent: NEMBUTAL (Dainippon Sumitomo Pharma Co., Ltd., Osaka, Japan), Adhesive agent (Aron Alpha) (Daiichi Sankyo Co., Ltd., Tokyo, Japan).
5. Ultrasound equipments and probes for gene delivery – Ultrasound equipments: Sonopore 3000 and Sonopore 4000 (NEPAGENE Co. Ltd.), Probe: KP-T6 (diameter: 6 mm) and KP-T8 (diameter: 8 mm), KP-T20 (diameter: 20 mm) (NEPAGENE Co., Ltd.)
6. Assessment of cytotoxicity: MTT [3-(4,5-s-dimethylthiazol-2-yl)-2,5-diphenyl tetrazolium bromide] (Dojindo, Kumamoto, Japan), Sodium dodecyl sulfate (SDS) (Wako Pure Chemical Industries), Microplate reader (POWERSCAN HT; Dainippon Pharmaceutical, Osaka, Japan).
7. Luciferase assay: Cell lysis buffer (0.1 M Tris–HCl (pH 7.8), 0.1% Triton X-100, 2 mM EDTA), Luciferase assay system (Promega, Madison, WI), Luminometer (TD-20/20) (Turner Designs, Sunnyvale, CA).
8. In vivo luciferase imaging: Escain (Mylan Inc., Tokyo, Japan), D-luciferin and In vivo luciferase imaging system (IVIS) (Caliper Life Sciences, MA).

3. Methods

3.1. Preparation of BLs (18)

1. DSPC and DSPE-PEG(2 k)-OMe were dissolved in 8 mL of 1:1 (v/v) chloroform/diisopropyl ether.
2. Four milliliter of PBS (pH 7.4) was added into the lipid solution. The mixture was sonicated to make suspension, and evaporated at 65° (water bath) to remove solvent.
3. After evaporation, liposome suspension was passed through sizing filters (pore sizes: 100 and 200 nm) using an extruding apparatus. And the size of liposomes was adjusted to less than 200 nm.
4. The liposomes suspension was sterilized by passing them through a 0.45 μm pore size filter. (see Fig. 1a)
5. Finally, size of the sterilized liposomes was measured with dynamic light scattering (ELS-800). The average diameter of

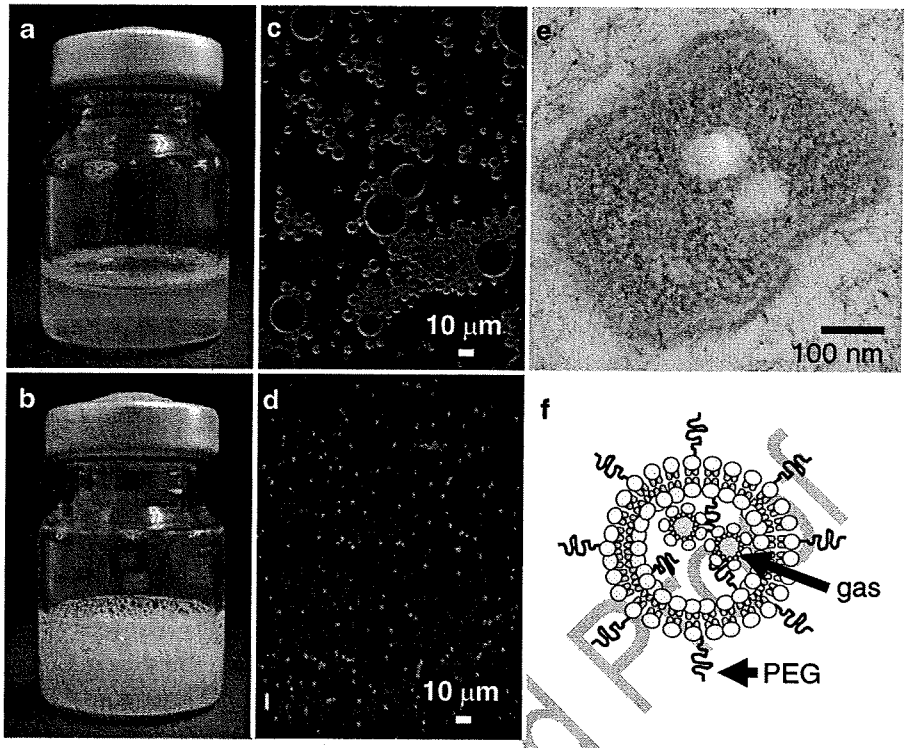

Fig. 1. Aspect and structure of BLs. PEG-liposomes (**a**) were sonicated with supercharged perfluoropropane gas. After that, they became to BLs (**b**). Optison (**c**) and BLs (**d**) were observed with microscope using the darklite illuminator (NEPAGENE, Co., Ltd). (**e**): Transmission electron microscopy (TEM) of BLs. (**f**): Scheme of structure of BLs

these liposomes were about 150–200 nm. In addition, lipid concentration was measured with the Phospholipid C-test wako.

6. The lipid concentration of liposomes suspension was adjusted to 1 mg/mL with PBS.
7. Two milliliter of the liposomes suspension (lipid conc. 1 mg/mL) was entered into sterilized vial (vial size: 5 mL).
8. The vial was filled with perfluoropropane, capped and then supercharged with 7.5 mL of perfluoropropane.
9. The vial was placed in a bath-type sonicator (42 kHz, 100 W) for 5 min to form BLs (see Fig. 1 and Note 1).

3.2. Transmission Electron Microscopy of BLs (20)

1. BLs were suspended into sodium alginate (500-600cP) solution (0.2% (w/v) in PBS).
2. This suspension was dropped into calcium chloride solution (100 mM in PBS) to hold BLs within calcium alginate gel.
3. The beads of calcium alginate gel containing BLs were prefixed with 2% glutaraldehyde solution in 0.1 M Cacodylate buffer.
4. The beads were postfixed with 2% OsO_4, dehydrated with an ethanol series, and then embedded in Epan812 (polymerized at 60°).

5. Ultrathin sections were made with an ultramicrotome at a thickness of 60–80 nm.
6. Ultrathin sections were mounted on 200 mesh copper grids.
7. They were stained with 2% uranyl acetate for 5 min and Pb for 5 min.
8. The samples were observed with JEOL JEM12000EX at 100 kV (see Fig. 1e; Notes 2 and 3).

3.3. In Vitro Ultrasonography with BLs (19)

1. BLs were placed into latex tube filled with degassed PBS (10 mL) in a water bath.
2. The probe (9 MHz) of an ultrasound imaging equipment was positioned under the water bath.
3. BLs in the tube were imaged (see Fig. 2 a, b).

3.4. In Vitro Gene Delivery with BLs and US

3.4.1. Transfection of Plasmid DNA into Cells with BLs and US (21)

1. Plasmid DNA, cells and BLs were suspended in culture medium with 10% FBS (final volume; 500 μL) in 2 mL polypropylene tubes.
2. The probe (KP-T6) (2 MHz, diameter: 6 mm) of US was placed into the suspension.
3. US was exposed to the suspensions with Sonopore 3000 or 4000 under the condition of various US parameters (Duty, Intensity, Exposure time, Burst rate) (see Fig. 2c).

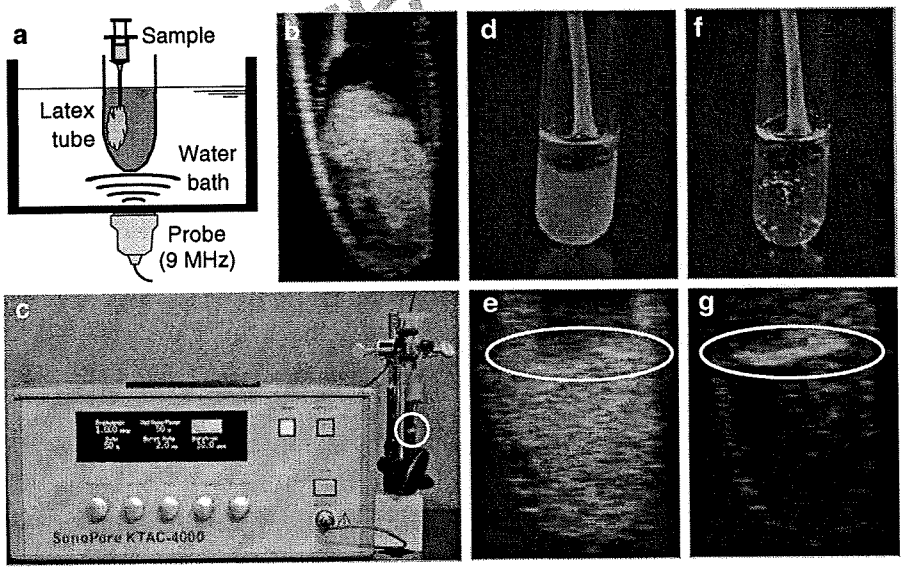

Fig. 2. In vitro Ultrasonography with BLs. The Method of ultrasonography for observation of BLs was shown in (**a**). BLs were injected into PBS filled latex tube in the water bath. Then, the samples were observed with ultrasonography (**b**). To confirm the disruption of BLs by US exposure using Sonopore 4000 (**c**), BLs were observed with naked image (**d**, **f**) and ultrasonography (**e**, **g**) before (**d**, **e**) and after (**f**, **g**) US exposure (2 MHz, 2.5 W/cm^2, 10 s). *Circle* in (**c**, **e**, **g**) shows US probe

4. After US exposure, the cells were washed twice with PBS and then resuspended in fresh culture medium.
5. The cells were cultured in culture plate or wells.
6. After 2 days culture of cells, the expression of transgene was measured (see Fig. 3; Notes 4 and 5).

3.4.2. Assessment of Cytotoxicity by the Treatment of BLs and US to Cells (18)

1. Cells (1×10^5) and BLs were suspended in culture medium with 10% FBS (final volume; 500 μL) in 2 mL polypropylene tubes.
2. US was exposed to cells using Sonopore 3000 or 4000 with a probe (KP-T6) (2 MHz, diameter: 6 mm).
3. After US exposure, the cells were washed twice with PBS and then resuspended in fresh culture medium.
4. One hundred microliter of the cells suspension were cultured in 96 well plates for 24 h.
5. Cell viability was assayed using MTT, as described by Mosmann, with minor modifications (22). Briefly, MTT (5 mg/mL, 10 μL) was added to each well, and the cells were incubated at 37°C for 4 h. The formazan product was dissolved in 100 μL of 10% SDS containing 15 mM HCl. Color intensity was measured using a microplate reader at test and reference wavelengths of 595 and 655 nm, respectively.

3.5. In Vivo Gene Delivery with BLs and US

3.5.1. Gene Delivery for Femoral Artery (18)

1. The femoral artery was exposed by operation.
2. BLs (250 μg) and plasmid DNA (10 μg) suspension (300 μL) was slowly injected into the femoral artery of ddY mice (6 weeks age, male) using 30-gauge needle (M-S Surgical MFG. Co. Ltd., Tokyo, Japan).
3. In the same time, US (frequency: 1 MHz, duty: 50%, intensity: 1 W/cm^2, time: 2 min) was transdermally exposed to downstream of injection site using Sonopore 3000 or 4000 with a probe (KP-T8) (diameter: 8 mm). [AU1]
4. After 2 days of injection, the mice were sacrificed and the femoral artery of US exposure area was collected. Then, gene expression in the artery was measured (see Fig. 4; Notes 6 and 7).

3.5.2. Gene Delivery for Ascites Tumor (20)

1. S-180 cells (1×10^6 cells) were i.p. injected into ddY mice (4 weeks age, male) on day 0.
2. When S-180 cells grew as the ascites tumor in mice after 8 days of the injection, the mice were anaesthetized with NEMBUTAL Injection (50 mg/kg), then injected with 510 μL of plasmid DNA and BLs (500 μg) in PBS.
3. US (frequency: 1 MHz, duty: 50%, intensity: 1 W/cm^2, time: 1 min) was transdermally exposed to the abdominal area using Sonopore 300 or 4000 with a probe (KP-S20) (diameter: 20 mm).

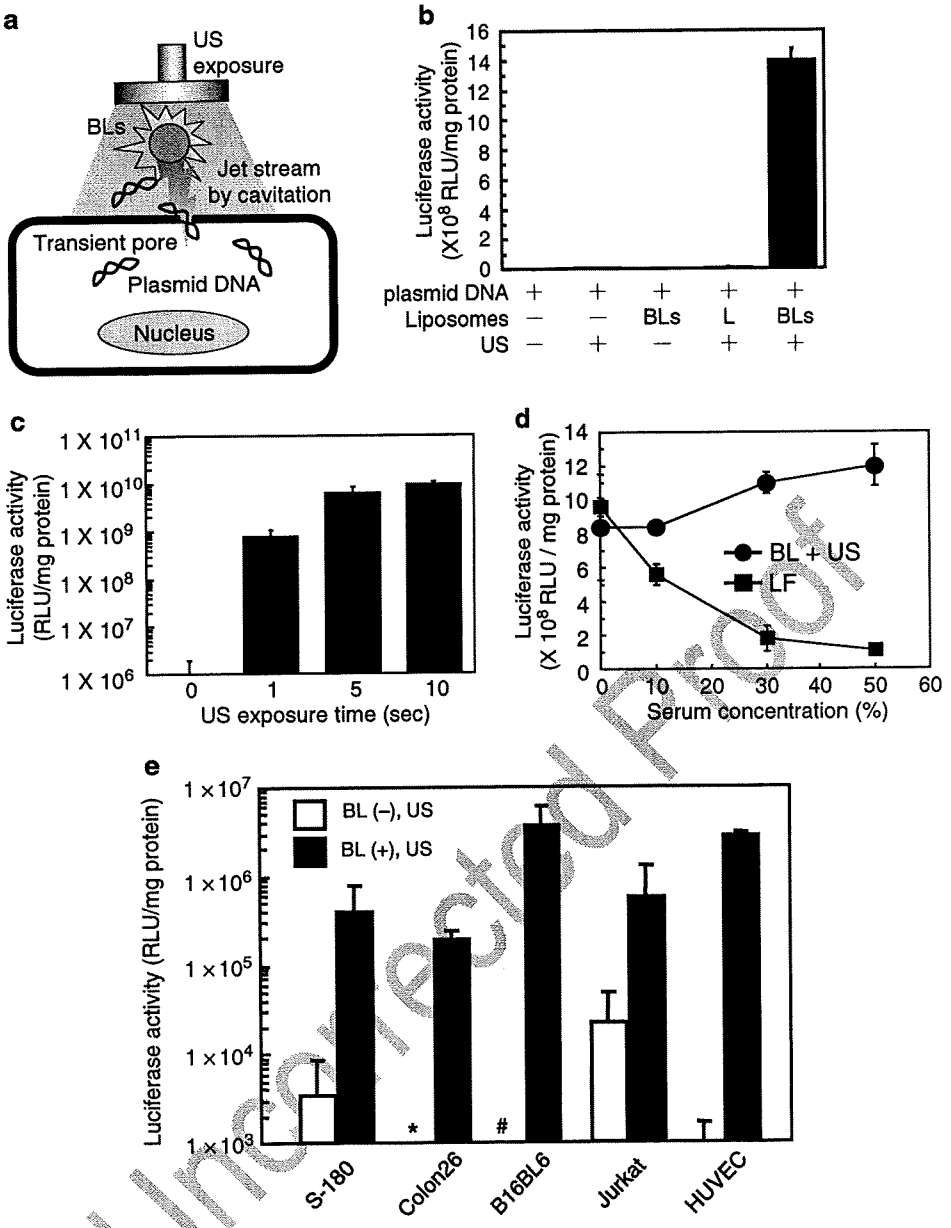

Fig. 3. Property of gene delivery with BLs and US exposure (**a**) Schema of transfection mechanism by BLs and US. The mechanical effect based on the disruption of BLs by US exposure, which results in generation of some pores on plasma membrane, is associated with direct delivery of extracellular plasmid DNA into cytosol. (**b**) Luciferase expression in COS-7 cells transfected by BLs and US. COS-7 cells (1×10^5 cells/500 μL/tube) were mixed with pCMV-Luc (5 μg) and BLs (60 μg). The cell mixture was exposed with US (Frequency: 2 MHz, Duty: 50%, Burst rate: 2 Hz, Intensity: 2.5 W/cm², Time: 10 s). The cells were washed and cultured for 2 days. After that, luciferase activity was measured. (**c**) Effect of US condition on transfection efficiency with BLs. COS-7 cells were exposed with US (Frequency: 2 MHz, Duty: 50%, Burst rate: 2 Hz, Intensity: 2.5 W/cm², Time: 0, 1, 5, 10 s) in the presence of pCMV-Luc (0.25 μg) and BLs (60 μg). Luciferase activity was measured as above. (**d**) Effect of serum on transfection efficiency of BLs. COS-7 cells in the medium containing FBS (0, 10, 30, 50% (v/v)) were treated with US (Frequency: 2 MHz, Duty: 50%, Burst rate: 2 Hz, Intensity: 2.5 W/cm², Time: 10 s), pCMV-Luc (0.25 μg) and BLs (60 μg) or transfected with lipoplex of pCMV-Luc (0.25 μg) and lipofectin (1.25 μg). (**e**) In vitro gene delivery to various types of cell using BLs and US. The method of gene delivery was same as above. S-180: mouse sarcoma cells, Colon26: mouse colon adenocarcinoma cells, B16BL6: mouse melanoma cells, Jurkat: human T cell line, HUVEC: human umbilical endothelial cells. Luciferase activity was measured as above. * $<10^3$RLU/mg protein, # $<10^0$RLU/mg protein Each data represents the mean ± S.D. ($n=3$). L: PEG-liposomes, LF: Lipofectin

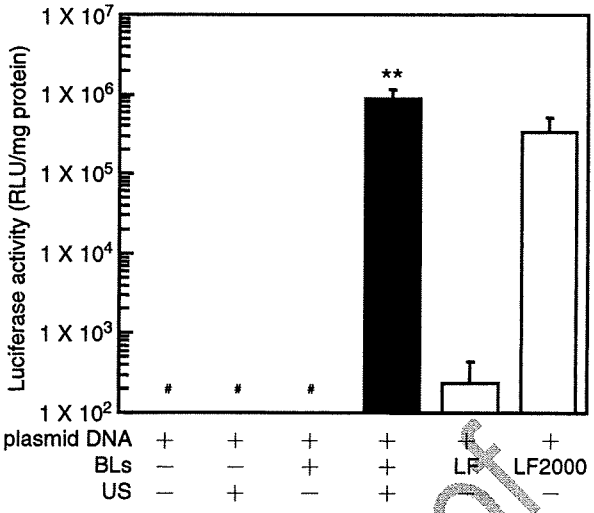

Fig. 4. In vivo gene delivery into mouse ascites tumor cells with Bubble liposomes. S-180 cells (1×10^6 cells) were i.p. injected into ddY mice. After 8 days, the mice were anaesthetized, then injected with 510 μL of pCMV-Luc (10 μg) and Bubble liposomes (500 μg) in PBS. Ultrasound (frequency: 1 MHz, duty: 50%; intensity: 1.0 W/cm^2, time: 1 min) was transdermally applied to the abdominal area. In another experiment, pCMV-Luc (10 μg) – Lipofectin (50 μg) or Lipofectamine 2000 (50 μg) complex was suspended in PBS (510 μL) and injected into the peritoneal cavity of mice. After 2 days, S-180 cells were recovered from the abdomens of the mice. Luciferase activity was determined, as described in Materials and Methods. Each bar represents the mean ± S.D. ($n = 3$–6). **$P < 0.01$ compared to the group treated with plasmid DNA, Bubble liposomes, ultrasound exposure or lipofection with Lipofectin or Lipofectamine 2000. LF, Lipofectin. LF2000, Lipofectamine 2000. # < 10^2 RLU/mg protein

4. After 2 days of US exposure, ascites tumor cells were recovered from the abdomen of the mice. Then, the gene expression in the recovered cells was measured (see Fig. 5).

3.5.3. Gene Delivery for Solid Tumor (20)

1. S-180 cells (1×10^6 cells) were inoculated into the left footpad of ddY mice (5 weeks age, male).
2. At day 4, when the thickness of the footpad was over 3.5 mm (normal thickness was about 2 mm), the left femoral artery was exposed by operation.
3. BLs (100 μg) and plasmid DNA suspension (100 μL) were injected into the femoral artery using 30-gauge needle.
4. In the same time, US (frequency: 0.7 MHz, duty: 50%, intensity: 1.2 W/cm^2, time: 2 min) was transdermally exposed to the tumor tissue using Sonopore 3000 or 4000 with a probe (KP-T8) (diameter: 8 mm).
5. The needle hole was then closed with an adhesive agent and skin was put in a suture.

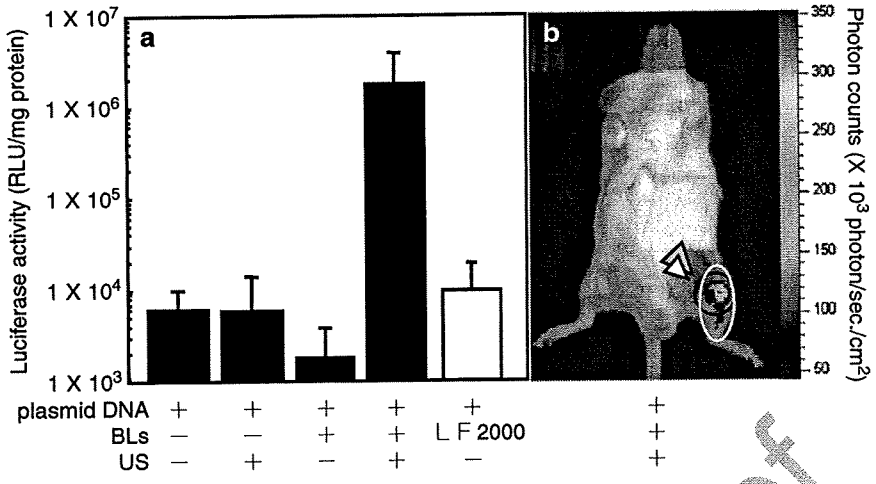

Fig. 5. Gene delivery to femoral artery with Bubble liposomes Each sample containing plasmid DNA 10 μg was injected into femoral artery. At the same time, ultrasound (frequency, 1 MHz; duty, 50%; burst rate, 2 Hz; intensity, 1 W/cm^2; time 2 min) was exposed to the downstream area of injection site. **(a)** Luciferase expression in femoral artery of the ultrasound exposure area at 2 days after transfection, Luciferase expression was determined as described in Materials and Methods. Data are shown as means ± S.D. (n=5). (LF2000: Lipofectamine 2000) **(b)** In vivo luciferase imaging at 2 days after transfection in the mouse treated with plasmid DNA, Bubble liposomes and ultrasound exposure. The photon counts are indicated by the pseudocolor scales

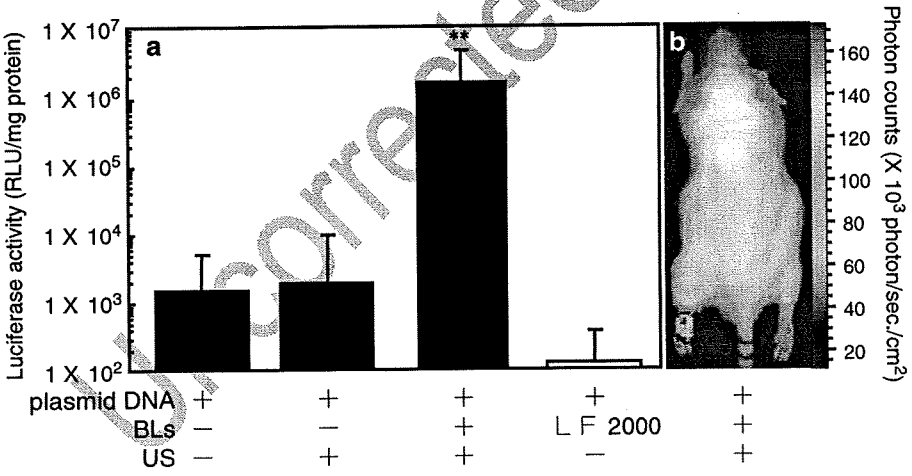

Fig. 6. In vivo gene delivery into mouse solid tumor with Bubble liposomes. S-180 cells (1×10^6 cells) were inoculated into left footpad of ddY mice. After 4 days, the mice were anaesthetized, then injected with 100 μL of pCMV-Luc (10 μg) in absence or presence of Bubble liposomes (100 μg) in PBS. Ultrasound (frequency: 0.7 MHz, duty: 50%; intensity: 1.2 W/cm^2, time: 1 min) was transdermally exposed to tumor tissue. In another experiment, pCMV-Luc (10 μg) – Lipofectamine 2000 (25 μg) complex was suspended in PBS (100 μL) and injected into the left femoral artery. After 2 days, tumor tissue was recovered from the mice. Luciferase activity was determined as described in Materials and Methods. **(a)** Luciferase activity in solid tumor. Each bar represents the mean ± S.D. for five mice/group. $^{**}P<0.01$ compared to the group treated with plasmid DNA, ultrasound exposure or Lipofectamine 2000. **(b)** In vivo luciferase imaging in the solid tumor bearing mice. The photon counts are indicated by the pseudocolor scales. LF 2000, Lipofectamine 2000

6. After 2 days of US exposure, the mice were sacrificed and the tumor tissues were collected. Then, the gene expression of the tumor tissue was measured (see Fig. 6 and Note 8).

3.6. Measurement of Reporter Gene Expression

3.6.1. Luciferase Assay

1. The lysis buffer (0.1 M Tris–HCl (pH 7.8), 0.1% Triton X-100, 2 mM EDTA) was added to the sample cells in vitro or tissues in vivo. In the case of the tissues in vivo, they were homogenized before next step.
2. The cells or the homogenized tissues in lysis buffer were repeatedly frozen and thawed three times to completely disrupt the cell membranes.
3. After that, the lysate of the cells or tissues was centrifuged and the supernatant was collected in other tube.
4. Luciferase activity in the supernatant was measured using a luciferase assay system and a luminometer. The activity is reported in relative light units (RLU) per mg protein of cells or tissue.

3.6.2. In Vivo Luciferase Imaging

1. The mice were anaesthetized with Escain and i.p. injected with D-luciferin (150 mg/kg).
2. After 10 min, luciferase expression was observed with in vivo luciferase imaging system (IVIS).

4. Notes

1. There are some important points to prepare BLs. The air in the vial containing the liposome suspension is completely replaced with perfluoropropane. After that, it needs to be supercharged in the vial with perfluoropropane. And the vial is sonicated with a bath-type sonicator (42 KHz, 100 W) (BRANSONIC 2510 J-DTH, Branson Ultrasonics). In this step, sonication power and the vial position in the bath are very important. Because we have experimented that BLs were not prepared using other type of bath sonicator (UC-1 (38 KHz, 80 W), IKEDA RIKA, Japan) with low intensity of ultrasound exposure. In addition, BLs were not prepared using other gas such as air, nitrogen gas or carbonic dioxide gas. Therefore, it thought that it is important for the preparation of BL to use hydrophobic gas such as perfluoropropane.
2. To fix BLs as a sample for transmission electron microscope, BLs were held within calcium alginate gel. The handling of BLs was improved by holding within the gel. The advantage for using this gel is to make the gel even at low temperature. Because BLs became unstable according to increasing temperature. Therefore, it is thought that the gel, such as agarose, which has gel point at high temperature is inappropriate for this purpose.
3. It was thought that liposomes were reconstituted by sonication under the condition of supercharge with perfluoropropane.

Then, perfluoropropane was entrapped within lipids like micelles. In addition, the lipid nanobubbles were encapsulated within liposomes. To confirm the structure of BLs, we observed BLs with transmission electron microscope. Interestingly, BLs had nanobubbles into lipid bilayer. Therefore, we called this "Bubble liposome" because of this structure. This structure of BLs was different from that of conventional microbubbles and nanobubbles which had lipid monolayer.

4. This protocol can be adapted for many other types of cell. In the gene transfection for adherent cells, the transfection efficiency in the condition of suspension was higher than that in the condition of adhesion on the culture plate. Although this result is unclear, it is thought that the distance between BLs and cells is important. Because BLs entrapping gas is easy to flow and result in getting away from the adherent cells on the plate.
5. In in vitro gene delivery, it is very important to fix the location of it, in order to reduce the experimental error of each data. The efficiency of this gene delivery was not affected even in the presence of serum. Moreover, the gene expression was observed even under the condition of US exposure for 1 s. From these results, it was suggested that this system could immediately deliver plasmid DNA into cells.
6. In in vivo gene delivery, echo jelly is necessary for US exposure to mice. Gene expression was observed in the arrested area of US exposure. Because it is thought that the mechanical effect based on the disruption of BLs by US exposure results in generation of some pores on plasma membrane of the cells in the area of US exposure.
7. This system is thought that there is not a serious damage for the cells in blood such as red blood cells by the disruption of BLs in blood stream by US exposure.
8. The transfection efficiency with the gene delivery system by sonoporation mechanism using BLs and US was higher than conventional lipofection method with Lipofectin and Lipofectamine 2000. Therefore, it is expected that this system might be an effective nonviral gene delivery system.

Acknowledgements

We are grateful to Dr. Katsuro Tachibana (Department of Anatomy, School of Medicine, Fukuoka University) for technical advice regarding the induction of cavitation with ultrasound, to Dr. Naoki Utoguchi, Mr. Yusuke Oda, Mr. Eisuke Namai,

Ms. Tomoko Takizawa, Ms. Kaori Sawamura and Ms. Kumiko Tanaka (Department of Pharmaceutics, School of Pharmaceutical Sciences, Teikyo University), Yoichi, Negishi (School of Pharmacy, Tokyo University of Pharmacy and Life Science), and Dr. Kosuke Hagisawa (Department of Medical Engineering, National Defense Medical College) for excellent technical advice and assistance, to Mr. Yasuhiko Hayakawa, Mr. Takahiro Yamauchi, and Mr. Kosho Suzuki (NEPAGENE Co., Ltd.) for technical advice regarding ultrasound exposure using Sonopore 3000 and 4000, and Sonitron 2000.

This study was supported by an Industrial Technology Research Grant in 2004 from NEDO, JSPS KAKENHI (16650126), MEXT KAKENHI (160700392, 19700423), a Research on Advanced Medical Technology (17070301) in Health and Labour Sciences Research Grants from Ministry of Health, Labour and Welfare, and the Program for Promotion of Fundamental Studies(07-24) in Health Sciences of the National Institute of Biomedical Innovation (NIBIO).

References

1. Fechheimer M, Boylan JF, Parker S, Sisken JE, Patel GL, Zimmer SG (1987) Transfection of mammalian cells with plasmid DNA by scrape loading and sonication loading. Proc Natl Acad Sci U S A 84:8463–8467
2. Miller MW, Miller DL, Brayman AA (1996) A review of in vitro bioeffects of inertial ultrasonic cavitation from a mechanistic perspective. Ultrasound Med Biol 22:1131–1154
3. Joersbo M, Brunstedt J (1990) Protein synthesis stimulated in sonicated sugar beet cells and protoplasts. Ultrasound Med Biol 16:719–724
4. Miller DL, Pislaru SV, Greenleaf JE (2002) Sonoporation: mechanical DNA delivery by ultrasonic cavitation. Somat Cell Mol Genet 27:115–134
5. Guzman HR, McNamara AJ, Nguyen DX, Prausnitz MR (2003) Bioeffects caused by changes in acoustic cavitation bubble density and cell concentration: a unified explanation based on cell-to-bubble ratio and blast radius. Ultrasound Med Biol 29:1211–1222
6. Wei W, Zheng-zhong B, Yong-jie W, Qing-wu Z, Ya-lin M (2004) Bioeffects of low-frequency ultrasonic gene delivery and safety on cell membrane permeability control. J Ultrasound Med 23:1569–1582
7. Duvshani-Eshet M, Machluf M (2005) Therapeutic ultrasound optimization for gene delivery: a key factor achieving nuclear DNA localization. J Control Release 108:513–528
8. Tata DB, Dunn F, Tindall DJ (1997) Selective clinical ultrasound signals mediate differential gene transfer and expression in two human prostate cancer cell lines: LnCap and PC-3. Biochem Biophys Res Commun 234:64–67
9. Kim HJ, Greenleaf JF, Kinnick RR, Bronk JT, Bolander ME (1996) Ultrasound-mediated transfection of mammalian cells. Hum Gene Ther 7:1339–1346
10. Greenleaf WJ, Bolander ME, Sarkar G, Goldring MB, Greenleaf JF (1998) Artificial cavitation nuclei significantly enhance acoustically induced cell transfection. Ultrasound Med Biol 24:587–595
11. Shohet RV, Chen S, Zhou YT, Wang Z, Meidell RS, Unger RH, Grayburn PA (2000) Echocardiographic destruction of albumin microbubbles directs gene delivery to the myocardium. Circulation 101:2554–2556
12. Taniyama Y, Tachibana K, Hiraoka K, Namba T, Yamasaki K, Hashiya N, Aoki M, Ogihara T, Yasufumi K, Morishita R (2002) Local delivery of plasmid DNA into rat carotid artery using ultrasound. Circulation 105:1233–1239
13. Taniyama Y, Tachibana K, Hiraoka K, Aoki M, Yamamoto S, Matsumoto K, Nakamura T, Ogihara T, Kaneda Y, Morishita R (2002) Development of safe and efficient novel nonviral gene transfer using ultrasound: enhancement of transfection efficiency of naked plasmid DNA in skeletal muscle. Gene Ther 9:372–380

14. Sonoda S, Tachibana K, Uchino E, Okubo A, Yamamoto M, Sakoda K, Hisatomi T, Sonoda KH, Negishi Y, Izumi Y, Takao S, Sakamoto T (2006) Gene transfer to corneal epithelium and keratocytes mediated by ultrasound with microbubbles. Invest Ophthalmol Vis Sci 47:558–564
15. Newman CM, Bettinger T (2007) Gene therapy progress and prospects: ultrasound for gene transfer. Gene Ther 14:465–475
16. Lindner JR (2004) Microbubbles in medical imaging: current applications and future directions. Nat Rev Drug Discov 3:527–532
17. Tsunoda S, Mazda O, Oda Y, Iida Y, Akabame S, Kishida, T, Shin-Ya M, Asada H, Gojo S, Imanishi J, Matsubara H, Yoshikawa T (2005) Sonoporation using microbubble BR14 promotes pDNA/siRNA transduction to murine heart. Biochem Biophys Res Commun 336:118–127
18. Suzuki R, Takizawa T, Negishi Y, Hagisawa K, Tanaka K, Sawamura K, Utoguchi N, Nishioka T, Maruyama K (2007) Gene delivery by combination of novel liposomal bubbles with perfluoropropane and ultrasound. J Control Release 117:130–136
19. Suzuki R, Takizawa T, Negishi Y, Utoguchi N, Maruyama K (2007) Effective gene delivery with liposomal bubbles and ultrasound as novel non-viral system. J Drug Target 15:531–537
20. Suzuki R, Takizawa T, Negishi Y, Utoguchi N, Sawamura K, Tanaka K, Namai E, Oda Y, Matsumura Y, Maruyama K (2008) Tumor specific ultrasound enhanced gene transfer in vivo with novel liposomal bubbles. J Control Release 125:137–144
21. Suzuki R, Takizawa T, Negishi Y, Utoguchi N, Maruyama K (2008) Effective gene delivery with novel liposomal bubbles and ultrasonic destruction technology. Int J Pharm 354:49–55
22. Mosmann T (1983) Rapid colorimetric assay for cellular growth and survival: application to proliferation and cytotoxicity assays. J Immunol Methods 65:55–63

Expert Opinion

Tight junction modulator and drug delivery

Koji Matsuhisa, Masuo Kondoh†, Azusa Takahashi & Kiyohito Yagi
Osaka University, Graduate School of Pharmaceutical Sciences, Department of Bio-Functional Molecular Chemistry, Osaka, Japan

Recent progress in pharmaceutical technology based on genomic and proteomic research has provided many drug candidates, including not only chemicals but peptides, antibodies and nucleic acids. These candidates do not show pharmaceutical activity without their absorption into systemic flow and movement from the systemic flow into the target tissue. Epithelial and endothelial cell sheets play a pivotal role in the barrier between internal and external body and tissues. Tight junctions (TJs) between adjacent epithelial cells limit the movement of molecules through the intercellular space in epithelial and endothelial cell sheets. Thus, a promising strategy for drug delivery is the modulation of TJ components to allow molecules to pass through the TJ-based cellular barriers. In this review, we discuss recent progress in the development of TJ modulators and the possibility of absorption enhancers and drug-delivery systems based on TJ components.

Keywords: absorption enhancer, claudin, drug delivery, occludin, paracellular route, tight junction

Expert Opin. Drug Deliv. (2009) 6(5):509-515

1. Introduction

Drug candidates, including chemicals, peptides, proteins, nucleic acids and their derivatives, can be efficiently identified by a combination of high-throughput technology and genome-based drug discovery. However, two steps are required for the clinical application of these drug candidates: movement of the molecules into the body and tissue through epithelial and endothelial cell sheets. These cell sheets regulate the movement of solutes between tissues within the body as well as between the outside and inside of the body.

Routes for passing of drug through the epithelial and endothelial cell sheets are classified into transcellular and paracellular routes (Figure 1). In the transcellular route, drugs are delivered by simple diffusion into the cell membranes and active transport via a receptor or transporter on the cell membrane [1,2]. Various transporters involved in the influx and efflux of peptides, organic anions and cations have been identified, and transcellular delivery systems using the transporters have been widely investigated [2-6]. Transporter-mediated drug delivery is tissue-specific and has low toxicity; however, the drugs must be modified for interaction with the transporter without loss of pharmaceutical activity. Thus, the transcellular route is not suitable for high-throughput production of drug candidates. The other route for drug delivery is the paracellular route. Tight junctions (TJs) seal the paracellular route and prevent the free movement of molecules in the paracellular space; therefore, a strategy for the paracellular delivery of drugs is the opening of TJs [7,8]. Compared with the transcellular route, the paracellular route has the advantages that drug modification is not needed and that one method can be applied for various drugs. Drug delivery systems through the paracellular route have been investigated as absorption enhancers since the 1980s. However, only sodium caprate is currently used as an absorption enhancer in pharmaceutical therapy.

10.1517/17425240902902315 © 2009 Informa UK Ltd ISSN 1742-5247

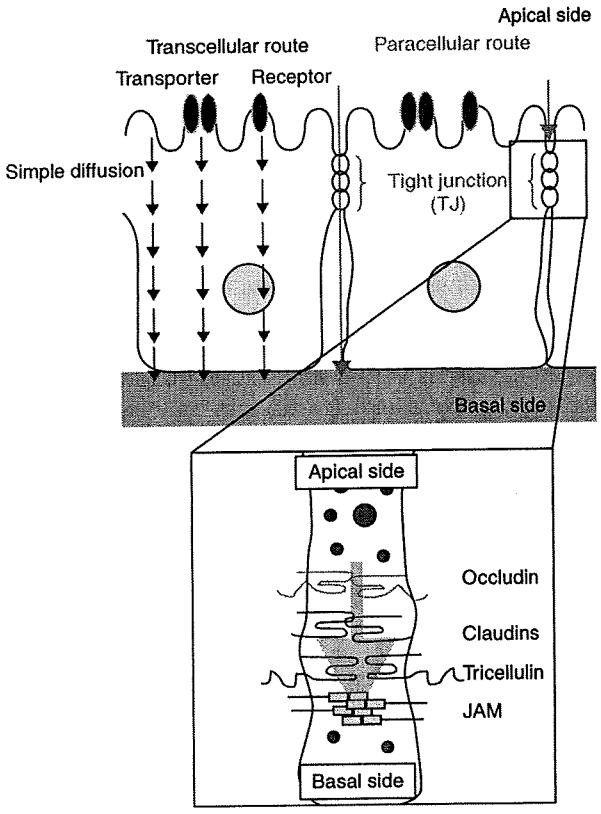

Figure 1. Schematic illustration of transport routes in epithelia.

It had been unclear how TJs regulated movement of solutes and what TJs were. In 1993, Furuse and colleagues determined that occludin, a protein with four transmembrane domains, is a component of TJs and that TJs consist of protein [9]. In 1998, Furuse and co-workers also identified another TJ protein, claudin-1 and -2 [10]. Claudins, a multigene family of at least 24 members, are key molecules of the TJ barrier [11]. Schematic biochemical machinery of TJs is shown in Figure 1, and modulation of the TJ components to allow drugs to pass through the paracellular route has been investigated as a novel strategy for drug delivery since the first report of TJ component-based drug delivery using an occludin peptide corresponding to part of the extracellular loop [12].

In this review, we examine recent topics in TJ-based drug delivery systems that use both approaches – TJ component/TJ modulator and TJ barrier – and discuss the future direction of such systems.

2. TJ components and TJ modulators

In the first section, we reviewed recent progress in TJ modulators over the past 2 years with respect to TJ components and modulators of TJ barrier.

2.1 Claudin

Claudin is a four-transmembrane TJ protein with a molecular mass of around 23 kDa, and comprises a family of at least 24 members [10]. Expression of each claudin member varies among cell types and tissues [13,14]. Claudins are thought to polymerize and form TJ strands in a homomeric and heteromeric manner, and the combination and mixing ratios of different claudin species determine the barrier properties of TJs, depending on the tissues [11]. For instance, deletion of claudin-1 causes dysfunction of the epidermal barrier [15], and deletion of claudin-5 causes dysfunction of the blood–brain barrier [16]. These findings indicate that a specific claudin modulator would be useful for tissue-specific drug delivery through the paracellular route. The C-terminal receptor binding region of *Clostridium perfringens* enterotoxin (C-CPE) is the only known modulator of claudin-4 [17]. Cells treated with C-CPE have decreased intracellular levels of claudin-4 as well as disrupted TJ barriers in epithelial cell sheets [17]. We previously found that the jejunal absorption-enhancing effect of C-CPE was 400-fold more potent than that of sodium caprate, the only clinically used absorption enhancer [18]. The development of other claudin modulators by using C-CPE as a prototype is a promising strategy. Deletion assays and site-directed mutagenesis assays indicate that the C-terminal 16 amino acids of C-CPE are involved in its modulation of claudin-4 and that Tyr residues at positions 306, 310 and 312 are critical for C-CPE activities [19,20]. Van Itallie and colleagues revealed that the structure of C-CPE is a nine-strand β sandwich and that the C-terminal 16–amino acid fragment is located in the loop region between the β8 and β9 strands, indicating that the claudin-4 binding site is on a large surface loop between strands β8 and β9 or on a domain containing these strands [21]. These findings indicate that peptides containing the loop structure formed by the β8 and β9 strands are likely to be novel claudin modulators. Considering the antigenicity of the claudin-4 modulator, smaller peptides are useful. Recently, the 12-mer peptide binders of claudin-4 were successfully identified using a random 12-mer peptide phage-display library [22]. The common claudin-binding motif <XX(Y/W)$(X)_{3\ or\ 4}$Y(Y/X)(L/I)XX> was also detected. The 12-mer peptide was bound to claudin with nanomolar affinity, but it did not modulate the claudin barrier. A 27-mer amino acid peptide corresponding to the extracellular loop region of claudin-1 modulated epithelial barrier through its interaction with claudin-3 [23]. Distinct species of claudins can interact within and between tight junctions [24]. Thus, a short peptide corresponding to the extracellular loop region of the heterotypically interacting claudin is also a candidate of claudin modulator.

2.2 Occludin

Occludin, a 65-kDa protein containing four transmembrane domains, was the first TJ-associated integral protein to be identified [9]. The initial strategy for TJ component-based

drug delivery was to use a synthetic peptide corresponding to the extracellular loop region of occludin *in vitro* [12]. The testes are rich in receptors for follicle-stimulating hormone. The effects of follicle-stimulating hormone-fused occludin peptide on the *in vivo* blood-testis barrier were investigated. The fusion protein modulated the blood–testis barrier, resulting in delivery of inulin into the testis [25]. Astrovirus infection causes diarrhea [26]. Moser and co-workers found that the astrovirus capsid disrupted occludin and increased the permeability of the TJ barrier without cytotoxicity in human intestinal cells [27]. A pro-inflammatory cytokine, IL-1β causes a functional opening of the intestinal TJ barrier without induction of apoptosis [28,29]. The IL-1β-induced enhancement of TJ permeability was mediated by downregulation of occludin through an increase in the myosin light chain kinase [29,30].

Thus, occludin peptides containing the ligand-targeting motifs and novel types of occludin modulators, such as the component capsid and the activator of myosin light chain kinase, may provide novel methods to deliver drugs into target tissues across endothelial cell sheets.

2.3 Ephrin

Ephrin-A2, a family of receptor tyrosine kinases, directly phosphorylates claudin-4 in epithelial cells, leading to the disruption of the epithelial barrier function [31]. Intravenous administration of ephrin-A2 ligand causes vascular permeability in the lungs, resulting in the leakage of albumin into the lungs of rats [32]. The ephrin-A2 ligand is altered in the disruption of the TJ barrier in the lungs of rats and in cultured lung vascular endothelial cells [32]. High levels of ephrin-A2 mRNA are also expressed in the intestine [33]. A modulator of the ephrin-A2 system will be a novel type of pulmonary and intestinal absorption enhancer.

2.4 Zonula occludens toxin

Zonula occludens toxin (Zot) is a 44.8-kDa envelope protein of *Vibrio cholera*, and zonulin is the intestinal Zot analogue that governs the permeability of intercellular TJs [34-36]. Zot and Zot derivatives are reversible TJ openers that enhance the delivery of drugs through the paracellular route without toxicity [35-40]. The Zots bind to a putative receptor on the apical surface of enterocytes, leading to protein kinase C-mediated polymerization of soluble G-actin and the subsequent loosening of TJs [38,41]. Zot enhanced the absorption of insulin in diabetic rats, and the bioavailability of oral insulin was sufficient to lower the serum glucose concentrations to an extent that was comparable to the parenteral injection of the hormone [35]. In 2001, an active fragment of Zot, ΔG with a molecular mass of 12 kDa, was identified [42]. In 2008, a hexapeptide derived from Zot, AT1002, was found to enhance absorption [43]. AT1002 increased permeability in human epithelial cell sheets without cytotoxicity and enhanced duodenal absorption of ciclosporin A.

2.5 Chitosan

Chitosan is derived from chitin, a polysaccharide found in the exoskeletons of insects, arachnids, and crustaceans. Chitosan is a nontoxic, biocompatible and mucoadhesive polymer that is a safe and efficient intestinal permeation enhancer for the absorption of drugs [44-46]. The chitosan-mediated activation of protein kinase Cα is followed by the redistribution of ZO-1 and an increase in TJ permeability, suggesting that the protein kinase Cα-dependent signal transduction pathway affects TJ integrity [47]. The oral administration of recently developed chitosan-coated nanoparticles containing insulin dramatically decreased blood glucose levels in diabetic rats [48].

2.6 HA, HAstV-1

Hemagglutinin (HA), a non-toxic component of the large 16S of the botulinum neurotoxin [49], and the human astrovirus serotype 1 (HAstV-1) capsid [27] may be a novel absorption enhancer via the paracellular route. The HA protein affected distribution of occludin, ZO-1, E-cadherin and β-catenin, and increased TJ permeability in human intestinal epithelial cells without cytotoxicity [49]. When HAstV-1 infected a Caco-2 cell monolayer from the apical side, the paracellular permeability was increased. UV-inactivated HAstV-1 also increased the permeability and disrupted occludin, indicating that the enhancement of the permeability was not dependent on viral replication [27]. Further analysis of the mode of action of these toxin- and virus-derived enhancers will lead to the development of novel intestinal absorption enhancers.

3. Physiological barriers modulated by TJ modulators

In the second section, we overviewed recent progress in TJ modulators with respect to the barrier separating different body compartments.

3.1 Blood–brain barrier

The blood–brain barrier, which comprises endothelial cell sheets with extremely tight junctions, limits the diffusion of hydrophilic molecules between the bloodstream and brain. Many pharmaceutical chemicals developed for the treatment of brain disorders cannot be applied in clinical therapy because they do not pass through the blood–brain barrier. Methods to open or reversibly regulate the blood–brain barrier have been investigated. Blood–brain barrier modulation based on the infection mechanisms of HIV has been proposed. Disruption of TJs occurs in the brains of HIV-infected patients [50-52], and tat protein, which is released from HIV-infected cells, decreases ZO-1 levels at the cell–cell borders in brain microvascular endothelial cells [53]. Tat treatment reduced expression of occludin, ZO-1, and ZO-2 in human brain microvascular endothelial cells via caveolin-1 and Ras signaling. Other HIV-1-derived proteins, gp120 and Nef,

Table 1. Candidates of absorption enhancer.

Target barrier	Candidates
Intestinal barrier	C-CPE
	AT1002
	Ephrin
	Chitosan and its derivatives
	Haemagglutinin
	HAstV-1 capsid
	Spermine
Blood-brain barrier	HIV-1 tat
	Sodium caprate
	Nitric oxide
Nasal barrier	AT1002
	Sperminated gelatin
	FDFWITP
Blood-testis barrier	C-type natriuretic peptide
	domain I of laminin β3

C-CPE: C-terminal of Clostridium perfringens enterotoxin; HAstv-1: Human astirovirus serotype 1; HIV: Human immunodeficiency virus.

can change the expression of TJ proteins *in vitro* [54]. Cocaine [55-56], sodium caprate [57] and nitric oxide [58] also modulate the blood–brain barrier.

3.2 Blood–testis barrier

Disruption of the blood–testis barrier affects spermatogenesis; thus, junctional proteins, such as occludin, ZO-1, and N-cadherin, could be the primary targets for testicular toxicants [59]. Monophthalates (mono-*n*-butyl phthalate and mono-2-ethylhexyl phthalate) were recently shown to disrupt the inter-Sertoli TJs in rat [60]. Phthalates are used as plasticizing and suspension agents in personal care products, plastics, paints, and pesticides. Monophthalates reduced the TJ barrier in Sertoli cells and induced the disappearance of ZO-1 and F-actin from around the cell periphery. The expression of occludin mRNA was also suppressed in a dose-dependent manner. C-type natriuretic peptide is a novel regulator of blood–testis barrier dynamics [61]. C-type natriuretic peptide regulates blood pressure, blood volume, fat metabolism, bone growth, and steroidogenesis in the testis and also reduces the expression of N-cadherin, occludin, and JAM-A [62,63]. Laminin fragments can also modulate the blood–testis barrier [64]. Treatment of primary Sertoli cells with domain I of laminin β3 caused a dose-dependent reduction in β1-integrin, occludin and ZO-1 and a decrease in the blood–testis barrier. Domain IV of laminin γ3 also reduced the expression of β1-integrin, occludin and JAM-A.

3.3 Epithelial barrier

Intranasal delivery is a convenient, reliable, rapid, and noninvasive delivery approach for low-molecular-weight compounds, and intranasal absorption enhancers have been developed for improvement of the nasal absorption of therapeutic macromolecules. AT1002, a polypeptide derived from Zot, enhanced not only intestinal absorption, but also nasal absorption of hydrophilic markers, PEG4000 and inulin [65]. Sperminated gelatin is a nasal absorption enhancer of insulin; when intranasally delivered, it decreases the plasma glucose level [66]. Aminated gelatin enhanced absorption of protein drugs through mucosal membranes with negligible mucosal damage [67].

Phage display technology is a powerful method for the selection of peptide ligands [68,69]. Recently, novel TJ modulators were isolated by using a phage-display library [70]. TJ-bound peptides were screened by using confluent monolayer cell sheets that were treated with a calcium chelator, EGTA. The polypeptide FDFWITP was isolated as a TJ binder. FDFWITP and its derivative peptides modulated TJ barriers without cytotoxicity, and these TJ-modulating activities were reversible. Thus, the phage-display system is a promising and powerful tool for developing TJ modulators.

4. Expert opinion

Many TJ-associated integral proteins, including occludin, claudin, tricellulin, ZO-1, ZO-2 and ZO-3, have been identified. These proteins play pivotal roles in the regulation of solute movement via the paracellular route, indicating that TJ modulators can be promising methods to deliver drugs. Studies of claudin-deficient mice initially indicated the possibility of TJ component-based drug delivery. Claudin-1-deficient mice lose their epidermal barrier function against a tracer with a molecular weight of around 600 Da, [15], indicating that claudin-1 modulators can enhance the transdermal absorption of drugs. The transdermal route is an easy, painless, and noninvasive method for drug administration, and the claudin-1 modulators have been the subject of pharmaceutical research. Claudin-5-deficient mice lose their blood–brain barrier [16], and small molecules (< 800 Da) selectively passed across the blood–brain barrier. The claudin-5 modulator will be a candidate for the pharmaceutical therapy of brain diseases. We found that the intestinal absorption-enhancing effects of a claudin-4 modulator were 400-fold more potent than those of a clinically used absorption enhancer [18]. Disruption of occludin or tricellulin increases TJ permeability [12,25,71]. These findings strongly indicate that modulation of TJ is a promising method for drug delivery. Because TJ proteins are poor in antigenicity, it is difficult to develop antibodies against the extracellular domain, resulting in a severe delay in the development of TJ modulators. At this point, there have been two breakthroughs in the development of TJ modulators. The first breakthrough is the determination of the structure of the only known claudin modulator, C-CPE [21]. The second breakthrough is the establishment of an efficient phage-display method to isolate a novel peptide to bind TJ components [22]. We believe that the

development of a claudin modulator by using C-CPE as a prototype will be successful, and that a peptide type of TJ modulator will be prepared in the near future. We are also optimistic about the production of a novel TJ modulator based on fragments of toxins, viruses and natural products. These fragments appear to use a novel mechanism to modulate the TJ barrier, and further analysis of this novel type of TJ modulator may lead to the next generation of TJ modulators (**Table 1**).

Very recently, Lee and colleagues proposed the lipid-protein hybrid model for TJ that the TJ proteins by themselves, and in combination with the lipids, serve, in addition, essential roles in barrier function, indicating that a lipid modulator can be a TJ modulator [72]. Glycosylated sphingosine, oxidized lipids and ether lipids were identified as TJ modulators, and the displacement of claudins and occludin from lipid raft was involved in the absorption-enhancing effect of sodium caprate [73,74]. Future investigation of the lipid-protein hybrid model for TJ may be the third breakthrough in the development of TJ modulators.

Declaration of interest

The authors state no conflict of interest and have received no payment in the preparation of this manuscript.

Bibliography

Papers of special note have been highlighted as either of interest (•) or of cossiderab;e interest (••) to readers.

1. Majumdar S, Duvvuri S, Mitra AK. Membrane transporter/receptor-targeted prodrug design: strategies for human and veterinary drug development. Adv Drug Deliv Rev 2004;56:1437-52
2. Mizuno N, Niwa T, Yotsumoto Y, Sugiyama Y. Impact of drug transporter studies on drug discovery and development. Pharmacol Rev 2003;55:425-61
3. Inui KI, Masuda S, Saito H. Cellular and molecular aspects of drug transport in the kidney. Kidney Int 2000;58:944-58
4. Koepsell H. Organic cation transporters in intestine, kidney, liver, and brain. Annu Rev Physiol 1998;60:243-66
5. Meijer DK, Hooiveld GJ, Schinkel AH, et al. Transport mechanisms for cationic drugs and proteins in kidney, liver and intestine: implication for drug interactions and cell-specific drug delivery. Nephrol Dial Transplant 1999;4(Suppl 14):1-3
6. Van Aubel RA, Masereeuw R, Russel FG. Molecular pharmacology of renal organic anion transporters. Am J Physiol Renal Physiol 2000;279:F216-32
7. Anderson JM, Van Itallic CM. Tight junctions and the molecular basis for regulation of paracellular permeability. Am J Physiol 1995;269:G467-75
8. Powell DW. Barrier function of epithelia. Am J Physiol 1981;241:G275-88
9. Furuse M, Hirase T, Itoh M, et al. Occludin: a novel integral membrane protein localizing at tight junctions. J Cell Biol 1993;123:1777-88

• **The first paper to identify a component of tight junction.**

10. Furuse M, Fujita K, Hiiragi T, et al. Claudin-1 and -2: novel integral membrane proteins localizing at tight junctions with no sequence similarity to occludin. J Cell Biol 1998;141:1539-50

• **The first paper to identify a functional component of tight junction.**

11. Furuse M, Tsukita S. Claudins in occluding junctions of humans and flies. Trends Cell Biol 2006;16(4):181-8
12. Wong V, Gumbiner BM. A synthetic peptide corresponding to the extracellular domain of occludin perturbs the tight junction permeability barrier. J Cell Biol 1997;136(2):399-409
13. Van Itallie CM, Anderson JM. Claudins and epithelial paracellular transport. Annu Rev Physiol 2006;68:403-29
14. Morita K, Furuse M, Fujimoto K, Tsukita S. Claudin multigene family encoding four-transmembrane domain protein components of tight junction strands. Proc Natl Acad Sci USA 1999;96:511-6
15. Furuse M, Hata M, Furuse K, et al. Claudin-based tight junctions are crucial for the mammalian epidermal barrier: a lesson from claudin-1-deficient mice. J Cell Biol 2002;156:1099-111
16. Nitta T, Hata M, Gotoh S, et al. Size-selective loosening of the blood-brain barrier in claudin-5-deficient mice. J Cell Biol 2003;161:653-60
17. Sonoda N, Furuse M, Sasaki H, et al. Clostridium perfringens enterotoxin fragment removes specific claudins from tight junction strands: evidence for direct involvement of claudins in tight junction barrier. J Cell Biol 1999;147:195-204

•• **Shows the first experimental evidence that claudin is responsible for tight junction barrier.**

18. Kondoh M, Masuyama A, Takahashi A, et al. A novel strategy for the enhancement of drug absorption using a claudin modulator. Mol Pharmacol 2005;67:749-56
19. Takahashi A, Komiya E, Kakutani H, et al. Domain mapping of a claudin-4 modulator, the C-terminal region of C-terminal fragment of Clostridium perfringens enterotoxin, by site-directed mutagenesis. Biochem Pharmacol 2008;75:1639-48
20. Takahashi A, Kondoh M, Masuyama A, et al. Role of C-terminal regions of the C-terminal fragment of Clostridium perfringens enterotoxin in its interaction with claudin-4. J Control Release 2005;108:56-62
21. Van Itallie CM, Betts L, Smedley JG III, et al. Structure of the claudin-binding domain of Clostridium perfringens enterotoxin. J Biol Chem 2008;283:268-74

•• **The first paper about the structure of C-CPE.**

22. Ling J, Liao H, Clark R, et al. Structural constraints for the binding of short peptides to claudin-4 revealed by surface plasmon resonance. J Biol Chem 2008;283:30585-95
23. Mrsny RJ, Brown GT, Gerner-smidt K, et al. A key claudin extracellular loop domain is crucial for epithelial barrier integrity. Am J Pathol 2008;172:905-15
24. Furuse M, Sasaki H, Tsukita S. Manner of interaction of heterogeneous claudin species within and between tight junction strands. J Cell Biol 1999;147:891-903